Journal of Physics: Conference Series **2156** (2022) 012007 doi:10.1088/1742-6596/2156/1/012007

# Ultra-High energy cosmic rays

**Silvia Mollerach**

Centro Atómico Bariloche, Comisión Nacional de Energía Atómica
Consejo Nacional de Investigaciones Científicas y Técnicas (CONICET)
Av. Bustillo 9500, R8402AGP, Bariloche, Argentina

E-mail: mollerach@cab.cnea.gov.ar

**Abstract.** An overview of the status of the knowledge in the field of ultra-high energy cosmic rays is presented. The latest results on the spectrum, arrival direction distribution and composition measurements are summarized and some implications for the understanding of the cosmic ray origin and their propagation are discussed.

## 1. Introduction

Cosmic rays (CR) reach the Earth from outside the Solar system with a wide range of energies from $10^9$ eV to $10^{20}$ eV. Their spectrum has an overall fall close to $E^{-3}$, as can be seen in Figure 1. The main spectral features appearing are a steepening at few PeV, called the knee, and a hardening at few EeV (1 EeV = $10^{18}$ eV), called the ankle. The spectrum also shows a strong fall close to $10^{20}$ eV.

At lower energies, up to $\sim$ 100 TeV, it is possible to detect directly particles from space using detectors in satellites, balloons and in the International Space Station, and precise determinations of the mass and charge of the particle are possible [2]. At higher energies, the flux of particles is very low and CRs can only be detected indirectly through extensive air showers of secondary particles that develop as they traverse the atmosphere.

The main open questions in the field are where and how these cosmic particles have been accelerated and how they propagated to the Earth. We have to take into account that during their propagation the particles can interact with the radiation and matter present in the medium and they can be deflected by the magnetic fields. Thus, the energy, direction, and sometimes even the mass of the particles may change during propagation.

At the lower energies, where direct measurements are possible, detailed measurements of the spectrum of individual elements have been performed in recent years, as presented in this conference by the AMS Collaboration, giving an extraordinary input to the field [3]. At these energies, particles come from sources within our Galaxy, probably being accelerated in shock waves in Supernova explosions. At higher energies, to study for example the end of the Galactic CR spectrum and the extragalactic CRs, it is necessary to resort to indirect measurements that cannot determine the identity of the particles, and the nuclei can only be classified in broad mass groups. There is evidence that the highest energy CRs are of extragalactic origin, but the sources are still unknown. It is not yet established at which energy the transition from Galactic to extragalactic CR origin happens. The results of the KASCADE-Grande experiment [4] show a steepening in the spectrum of the light component of CRs at energies close to the knee, while that of the heavy component has a steepening at around $10^{17}$ eV, where there is another feature

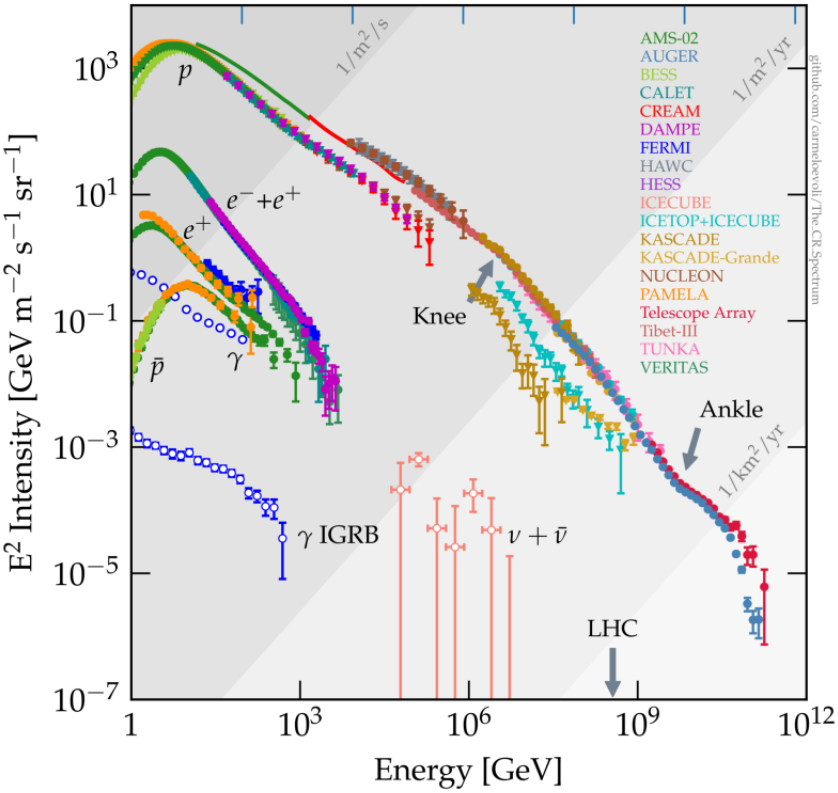


**Figure 1.** Energy flux ($E^2 d\Phi/dE$) of cosmic particles as measured by different experiments. The total spectrum, as well as those of different components, are shown (courtesy of C. Evoli [1])

of the spectrum called the second knee. These features can be interpreted as related to the end of the Galactic CR spectrum, with the light component starting to fade at the knee energy, while the heavy component starts to fade at the second knee. The underlying cause for the steepening, appearing at similar rigidities for different nuclei, could be the maximum rigidity of the acceleration process or a change in the propagation, with a higher escape rate from the Galaxy at high rigidities taking place.

## 2. Indirect cosmic ray measurements

Cosmic rays of high energy are detected through the extensive air showers produced when they interact in the atmosphere. These can be measured using an array of detectors that sample the particles reaching the ground. The largest observatory in operation is the Pierre Auger Observatory located in the Province of Mendoza (Argentina), composed of 1660 water-Cherenkov detectors covering 3000 km$^2$ and overlooked by 27 fluorescence detectors [5]. The largest observatory in the Northern hemisphere is the Telescope Array in Utah, USA, composed of 507 scintillators covering 700 km$^2$ and overlooked by 36 fluorescence detectors [6]. The fluorescence detectors measure the UV fluorescence light from nitrogen molecules excited by particles in the extensive air shower, producing a glow along their path in the atmosphere. On moonless nights, when the fluorescence detectors can be operated (with a duty cycle of $\sim 15\%$) the amount of deposited energy is measured as a function of the atmospheric depth. Its integral gives a calorimetric determination of the total energy of the shower, from which the energy of

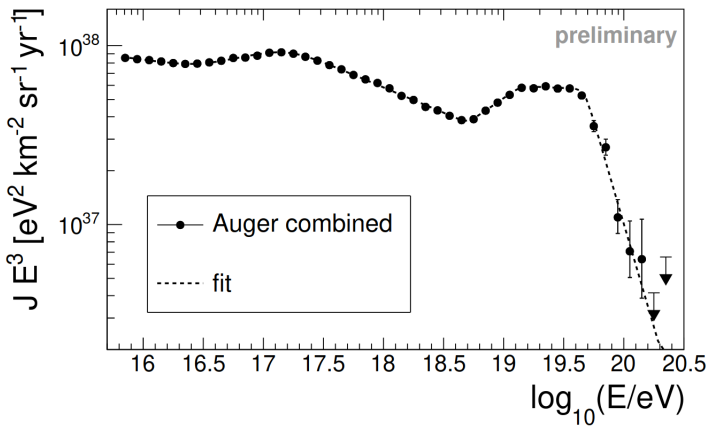


**Figure 2.** Spectrum of cosmic rays measured by the Pierre Auger Observatory [7].

the original particle can be estimated. On the other hand, the array of surface detectors sample with nearly 100% duty cycle the particles reaching the ground at different distances from the shower core. This allows a reconstruction of the CR arrival direction and a determination of the signal at a reference distance from the shower core, that for the Pierre Auger Observatory is chosen as 1000 m. This provides a good estimator of the energy of the primary particle, which can be calibrated with that measured by the fluorescence detectors for the fraction of the events measured by both detectors.

## 3. Spectrum and composition of ultra-high energy cosmic rays

The spectrum measured by the Pierre Auger Observatory is shown in Figure 2. The second knee at 0.16 EeV, presumably due to the fading of the heavy mass galactic component, is clearly seen. For increasing energies, the ankle hardening appears at 5 EeV, followed by a recently measured steeping at 14 EeV, called the instep, before the very strong steepening observed at 47 EeV.

A widely used mass composition indicator for extensive air showers is the atmospheric depth of the shower maximum, $X_{\rm max}$. This can be measured using the fluorescence detectors. Atmospheric showers initiated by a heavy nucleus develop higher in the atmosphere, and have smaller fluctuations than those initiated by lighter primaries. This can be understood as the superposition of smaller showers initiated by individual nucleons. Figure 3 shows the mean atmospheric depth $X_{\rm max}$ (left panel) and its dispersion (right panel) expected for p and Fe primaries for different hadronic interaction models together with the measurements by the Pierre Auger Observatory. The measurements indicate that the composition becomes lighter for increasing energies up to 2 EeV, and then it becomes heavier above this energy.

When we want to make contact between the spectrum and the composition of cosmic rays measured at the Earth and those of the accelerated particles at the sources, we have to take into account that CRs interact with the radiation backgrounds on their way to Earth. The main processes are pair production, photo-disintegration of nuclei and photo-pion production. For example, at $10^{20}$ eV a proton or an Fe nucleus needs to come from distances closer than $\sim 75$ Mpc, and nuclei with intermediate masses from even closer distances.

In order to interpret the observed spectrum and composition above the ankle with a simple model of uniformly distributed sources accelerating particles with a rigidity dependent spectrum (power law with exponential cutoff), the Pierre Auger Observatory results favour a scenario with a mixed composition at the sources [9], with a very hard spectrum and a rather low rigidity cutoff $R_{\rm cut} = E_{\rm cut}/Z \simeq 1.5$ EeV. As shown in Figure 4, increasingly heavier elements dominate

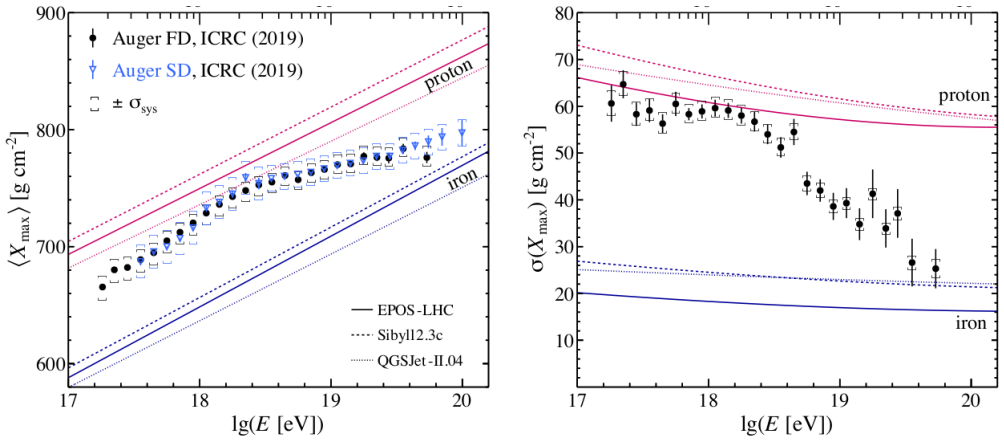


**Figure 3.** Measurements of the mean atmospheric depth of the shower maximum $X_{\max}$ and its dispersion from the Pierre Auger Observatory [8]. The expectations for p and Fe primaries for different hadronic interactions models are also displayed.

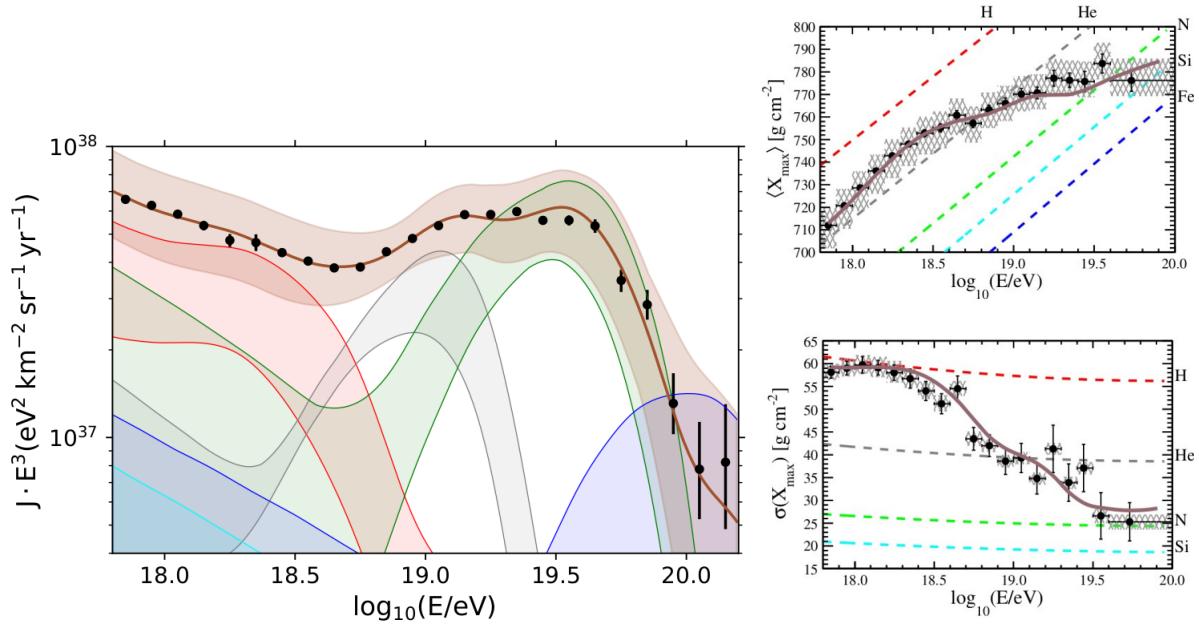


**Figure 4.** Combined spectrum and composition fit by the Pierre Auger Observatory. Left: The measured energy spectrum and the best fit results. The contribution of the different nuclei reaching the Earth are grouped according to their mass number: $A = 1$ (red), $2 \leq A \leq 4$ (grey), $5 \leq A \leq 22$ (green), $23 \leq A \leq 38$ (cyan), $39 \leq A$ (blue), with the bands accounting for the experimental uncertainties. Right: The first two moments of the $X_{\max}$ distributions in each energy bin along with their expected values and the predictions for pure compositions of H (red), He (grey), N (green), Si (cyan), Fe (blue) using the EPOS-LHC model [10].

the spectrum with increasing energies [9, 10]. To explain the measurements below the ankle a second component with a lighter composition and a softer spectrum is required [10]. The sources of this second component are also expected to be extragalactic in order to agree with the small

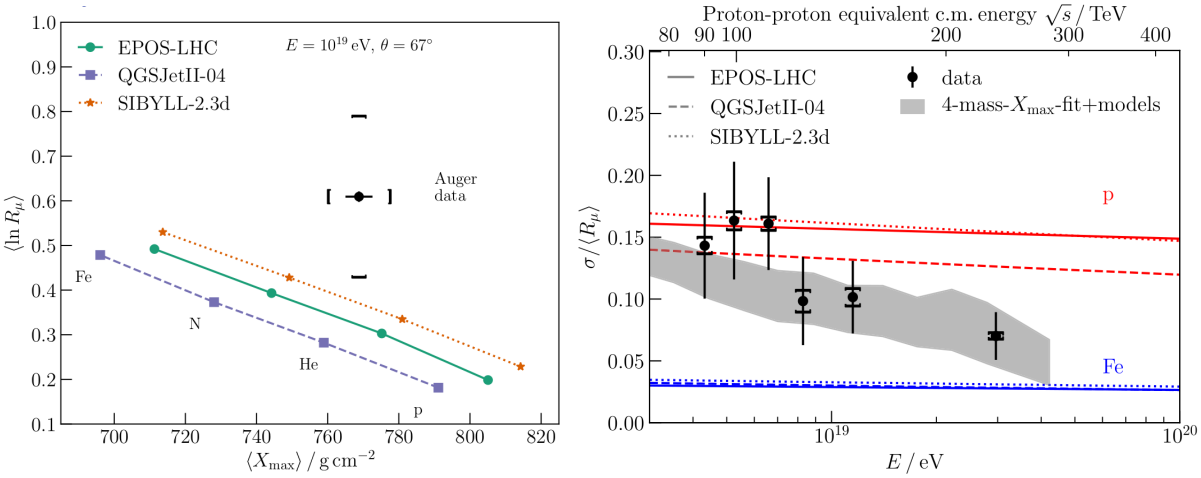


**Figure 5.** Left: expected muon density estimator and mean $X_{\rm max}$ for different composition and hadronic interaction models (lines) and the measurements from the Pierre Auger Observatory for energy $E = 10^{19}$ eV. Right: relative fluctuations in the number of muons as a function of energy [12, 13].

anisotropies observed in the distribution of the arrival directions at EeV energies. In this kind of scenario, the final steepening of the spectrum results from a combination of propagation effects and the maximum rigidity of the acceleration at the sources.

## 4. Hadronic interactions in air showers

Extensive air showers have essentially two parts, the electromagnetic component that is mainly produced by the decays of neutral pions, and the muonic component that comes mainly from the decays of charged pions. The electromagnetic one is the main component responsible for the atmospheric glow measured by the fluorescence detectors, and also contributes to the signals measured in the surface detectors. The muonic component contains a subdominant fraction of the shower energy, and can also give useful information about the primary particle mass composition. Higher mass primaries produce showers with more muons than lighter ones. A good theoretical model for the development of air showers should be able to describe consistently both the electromagnetic and the muonic parts. Muons are measured at the Pierre Auger Observatory by an array of underground scintillator detectors covering a small part of the surface array, that work in the energy range around $10^{18}$ eV [11]. They are also measured with the water-Cherenkov detectors by looking at the very inclined showers in which the electromagnetic component has been largely absorbed in the atmosphere, best suited in the energy range around $10^{19}$ eV. Measurements turn out to be slightly above the expectations even for Fe composition. Moreover, when we combine the $X_{\rm max}$ measurement with the muon measurements for the same energy bin, as shown in the left panel of Figure 5 for $E = 10^{19}$ eV, it is clear that none of the hadronic interactions models can consistently explain the observations for any composition [12]. Monte Carlo simulations of extensive air showers, considering the mass composition inferred from the $X_{\rm max}$ measurements, predict a muon density at ground smaller than the observed one for all the hadronic interaction models. On the other hand, the relative fluctuations in the number of muons, that mostly depend on the first interactions in the atmosphere, are in agreement with the expectations, as shown in the right panel of Figure 5. This is compatible with the muon deficit in the simulations originating from small deviations in the predictions from the hadronic interaction models that accumulate as the showers develop [13].

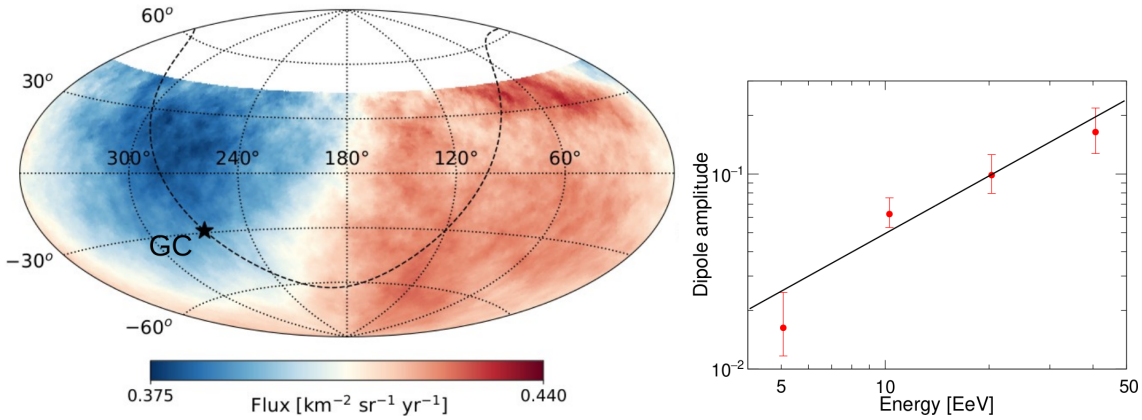


**Figure 6.** Flux of CRs with energies above 8 EeV smoothed in an angular scale of 45° (left panel) and amplitude of the dipolar component as a function of energy (right panel)[14]

## 5. Distribution of the arrival directions

At large angular scales, the Pierre Auger Observatory has measured a dipolar anisotropy with an amplitude of $d = 0.073^{+0.011}_{-0.009}$ in the arrival direction of CRs with energies above 8 EeV, that has a significance of $6.6\sigma$ [14]. The direction points to $(\alpha, \delta) = (95°, -36°)$, at 115° from the direction of the Galactic center. This is evidence of an extragalactic origin. The left panel of Figure 6 shows the flux smoothed in an angular window of 45° radius. The amplitude of the dipole is observed to be increasing with energy, as can be seen in the right panel of Figure 6. This is consistent with expectations, since particles of higher rigidity are less deflected by the magnetic fields and also because lower energy particles may arrive from farther away sources.

In the Northern hemisphere, Telescope Array has recently measured a modulation in right ascension of amplitude $r = 0.031 \pm 0.018$, pointing to $\alpha = 134° \pm 34°$ [6]. This amplitude corresponds to an equatorial dipole component $d_\perp = r/\langle\cos\delta\rangle \simeq 1.3\ r \simeq 0.04 \pm 0.02$, that is consistent with the Pierre Auger Observatory results ($d_\perp = 0.060 \pm 0.010$).

A combined analysis of the data from the two observatories, with full coverage of the sky, has also been performed [15]. First, a careful cross-calibration of the energies from both experiments has to be performed in order to avoid spurious modulations. This is possible by matching the spectra measured by the two observatories in the common declination band observed by both. The left panel of Figure 7 shows the flux smoothed in an angular window of 45° for an energy threshold of 8.57 EeV (Auger) and 10 EeV (TA). The combined dipole has an amplitude $d = 0.059 \pm 0.020$, and it is compatible with the Auger only results.

Regarding the large scale anisotropies at lower energies, the analysis of the right ascension distribution of the Pierre Auger Observatory data shows that the amplitude of the equatorial dipole component in the energy range from 0.1 EeV to 100 EeV grows from few $10^{-3}$ to about 10% in that energy range, and the phases show a change from being close to the right ascension of the Galactic center at low energies to nearly the opposite direction at the highest energies, suggesting a transition from anisotropies of Galactic origin below $\sim 1$ EeV to extragalactic origin above few EeV [16].

Looking at the anisotropies at higher energies and smaller angular scales, the most significant excess of flux in the Pierre Auger Observatory data happens above a threshold of 41 EeV and in an angular scale of 24°. The smoothed flux map is shown in the left panel of Figure 8. The post-trial significance of the excess is 2.2 $\sigma$ after taking into account the different energy thresholds, directions in the sky and angular windows probed [17]. The largest excess in the

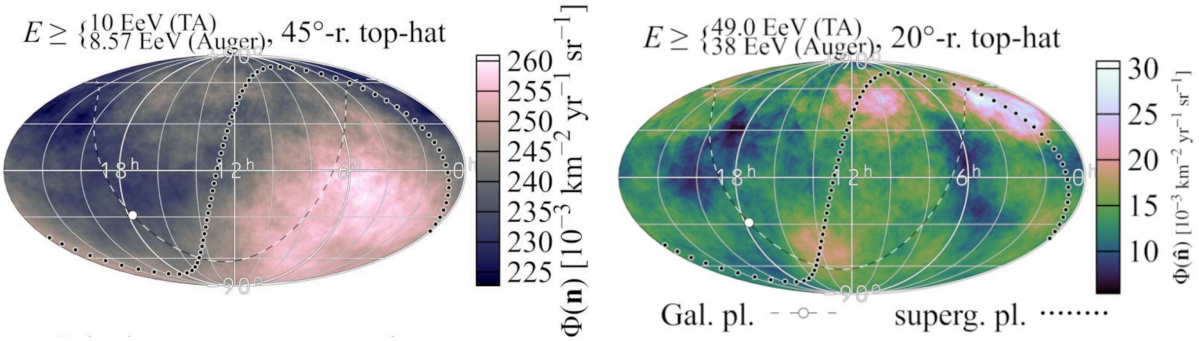


**Figure 7.** Maps of the flux in equatorial coordinates combining Pierre Auger Observatory and Telescope Array data. Left: flux of CRs smoothed in an angular window of 45° for an energy threshold of 8.57 EeV (Auger) and 10 EeV (TA).[15]. Right: flux smoothed in 20° window for an energy threshold of 38 EeV (Auger) and 49 EeV (TA). [18].

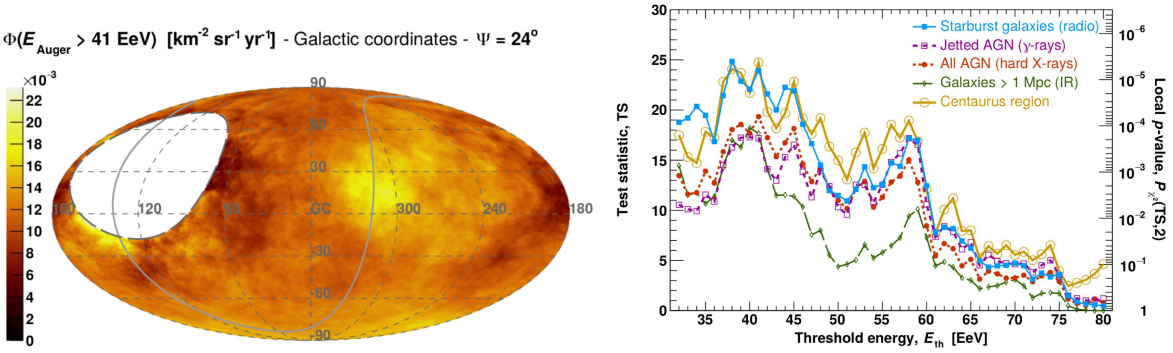


**Figure 8.** Left: The flux map in Galactic coordinates of UHECRs above 41 EeV smoothed with a top-hat window of radius 24° [17]. Right: The test statistic profile as a function of threshold energy for the four studied catalogs [13]. The local p-value, penalized for the search over the angular scale and signal fraction, is shown on the right-hand side axis. The profile of the local p-value for an overdensity in the Centaurus region, accounting for the scan in angle, is shown as a golden line.

Telescope Array data appears at $E > 57$ EeV and at an angular window of 25° with a post-trial significance of 3.2 $\sigma$ [6].

More constrained analyses around possible CR sources and against flux patterns expected from extragalactic object catalogs have also been performed by the Pierre Auger Observatory. An overdensity search centered on the radio-galaxy Centaurus A at $(l, b) = (309.5°, 19.4°)$ has a most significant excess of 56 events on top of 120 expected above a threshold energy of 41 EeV and within a radius of 27°, with a post-trial significance of 3.9 $\sigma$. Also the flux pattern expected from four catalogs representative of normal galaxies, starburst galaxies, all AGNs and jetted AGNs were investigated. The results are summarized in the right panel of Figure 8. The post-trial significances for deviation from isotropy range from 3.1 $\sigma$ (jetted AGN) up to 4.0 $\sigma$ (starbursts).

A similar analysis was performed with full sky coverage combining the data from the Pierre Auger and Telescope Array observatories using two catalogs representing the normal galaxy distribution within 250 Mpc and the starburst galaxies. A maximum test statistic of TS = 27.2

was obtained with the starburst catalog for an energy threshold of 38 EeV on the Auger scale (49 EeV on the TA scale). It has a post-trial significance of 4.2 $\sigma$. The combined flux map smoothed at an angular scale of 20° is shown in the right panel of Figure 7.

In summary, the distribution of the arrival directions of ultra-high energy cosmic rays shows a significant dipole above 8 EeV, there are some hints of medium scale anisotropies above 40 EeV and no evidence of small scale anisotropies. This is probably due to the fact that the deflections in the intergalactic magnetic field are significant. This is consistent with the transition to a heavier composition at the highest energies. This fact makes it difficult to identify the actual sources. There are several proposed source candidates that meet the minimal conditions for being accelerator sites, like AGNs, starburst galaxies, GRBs and magnetars, but the identification is difficult since the arrival directions of CRs do not point to their sources due to the magnetic deflections.

## 6. Conclusions

Several recent advances in the understanding of ultra-high energy CRs have been discussed, including the detailed measurements of the spectral features, the composition change to heavier elements at the highest energies and the dipolar anisotropy above 8 EeV, from which a consistent picture is starting to emerge. Despite this, the main question about the sources of UHECRs is still open. Major improvements in the two largest CR observatories currently taking place will help to enlighten it. The Pierre Auger Observatory is implementing an upgrade, AugerPrime, with the installation of plastic scintillators and radio antennas above all the water-Cherenkov detectors, with the aim to improve the sensitivity to the mass composition with 100 % duty cycle by measuring the muonic and electromagnetic components of every shower [19]. The Telescope Array is extending the area of the array (TA×4) to cover 3000 km$^2$ [6].

## Acknowledgments

This work was supported by CONICET (PIP 2015-0369) and ANPCyT (PICT 2016-0660).

## References

[1] C. Evoli, The Cosmic-Ray Energy Spectrum, https://doi.org/10.5281/zenodo.1468852
[2] V. Formato, TAUP 2021, this conference
[3] M. Paniccia, for the AMS Collaboration, TAUP 2021, this conference
[4] D. Kang, for the KASCADE-Grande Collaboration, PoS (ICRC 2019) 565
[5] A. Aab et al. (The Pierre Auger Collaboration), *Nucl. Instrum. Meth. A* **798** (2015) 172
[6] D. Bergman, for the Telescope Array Collaboration, TAUP 2021, this conference
[7] V. Novotny, for the Pierre Auger Collaboration, PoS (ICRC2021) 324; The Pierre Auger Collaboration, *Phys. Rev. Lett.* **125** (2020) 121106, *Phys. Rev. D* **102** (2020) 062005, *Eur. Phys. J. C* (2021) in press
[8] A. Yushkov, for the Pierre Auger Collaboration, PoS (ICRC2019)482; C. J. Todero Peixoto, for the Pierre Auger Collaboration, PoS (ICRC2019)440
[9] A. Aab et al. (The Pierre Auger Collaboration), JCAP04 (2017) 038, Err: JCAP 03 (2018) E02
[10] E. Guido, for the Pierre Auger Collaboration, PoS (ICRC2021)311
[11] A. Aab et al. (The Pierre Auger Collaboration), *Eur. Phys. J. C* (2020) 80:751
[12] The Pierre Auger Collaboration, *Phys. Rev. Lett.* **117** (2016) 192001, *Phys. Rev. D* **91**(2015)032003
[13] The Pierre Auger Collaboration, *Phys. Rev. Lett.* **126** (2021) 152002
[14] R. M. de Almeida, for the Pierre Auger Collaboration, PoS (ICRC2021) 335
[15] P. Tinyakov, for the Pierre Auger and Telescope Array Collaborations, PoS (ICRC2021) 375
[16] A. Aab et al. (The Pierre Auger Collaboration), *Astrophys. J.* **891** (2020) 142
[17] J. Biteau, for the Pierre Auger Collaboration, PoS (ICRC2021) 307
[18] A. di Matteo, for the Pierre Auger and Telescope Array Collaborations, PoS (ICRC2021) 308
[19] G. Cataldi, for the Pierre Auger Collaboration, PoS (ICRC2021)251; F. Schlüter, for the Pierre Auger Collaboration, PoS (ICRC2021)262